MRS Communications (2017), 7, 74–77
© Materials Research Society, 2017
doi:10.1557/mrc.2017.4

MRS Communications

Research Letter

Spray pyrolysis and electrochemical performance of $Na_{0.44}MnO_2$ for sodium-ion battery cathodes

Kuan-Yu Shen, Miklos Lengyel, Louis Wang, and **Richard L. Axelbaum,** Department of Energy, Environmental and Chemical Engineering, Washington University in St. Louis, One Brookings Drive, St. Louis, MO 63130, USA

Address all correspondence to R.L. Axelbaum at **axelbaum@wustl.edu**

(Received 27 November 2016; accepted 23 January 2017)

Abstract

In this study, we investigate spray pyrolysis as an approach to synthesis of tunnel structure sodium manganese oxide, as it is a cost-effective and scalable technology. The powders synthesized with Na/Mn ratio of 0.50 displayed a pure tunnel structure, and demonstrated the best electrochemical performance, with a discharge capacity of 115 mAh/g. The material also showed good cycleability and rate capability. Noticeable decay in performance was seen in materials with Na/Mn ratios other than 0.50, indicating that this material is sensitive to minor compositional deviations. This study has demonstrated that spray pyrolysis is a promising synthesis method for this material.

Introduction

Demand for large-scale energy storage solutions has been increasing as society reduces its dependence on fossil fuels. Lithium-ion batteries have been the dominant choice for energy storage for decades; however, there are concerns related to the limited availability of lithium, which could potentially increase costs and curtail large-scale implementation.[1,2] As a promising alternative, sodium-ion batteries have attracted significant attention in recent years. Sodium is one of the most abundant elements on earth and its related chemicals are significantly cheaper than the corresponding lithium ones.[3,4] Sodium is also the second-lightest and smallest alkali metal, next to lithium, thus minimizing the sacrifice in energy density, and allowing for more appealing economics. The potential markets for sodium-ion batteries include applications where cycle life and cost are more critical factors than energy density, such as grid-scale energy storage for smart grid applications.[2–4]

Among all the sodium-ion battery cathode materials, $Na_{0.44}MnO_2$ ($Na_4Mn_9O_{18}$) is particularly attractive due to its wide tunnel crystal structure, which is suitable for sodium intercalation. The manganese ions in $Na_{0.44}MnO_2$ are dispersed in octahedral sites (MnO_6) and a square-pyramidal environment (MnO_5).[5] The lattice forms two double and one triple octahedral chains, which results in two different types of three-dimensional tunnels. Two active sodium sites are situated in large S-shape tunnels, while the other inactive site is found in smaller tunnels. When fully charged, only the inactive site in smaller tunnels is filled with sodium, which leads to a theoretical capacity of 121 mAh/g. In 2007, Sauvage et al. studied $Na_{0.44}MnO_2$ and recorded at least five biphasic phenomena between 2 and 3.8 V at a slow rate of 1/200 C.[5] Hosono et al. improved the cycleability and retained 100 mAh/g at 0.42 C after 20 cycles.[6] Zhao et al. synthesized $Na_{0.44}MnO_2$ with carbon nanotubes in an attempt to increase rate performance.[7] The material demonstrated a capacity of 110 mAh/g at 0.5 C with almost no loss after 40 cycles. More recently, Wang et al. improved the material with a Ti substitution for part of the manganese. The material can be used as a negative electrode for aqueous sodium-ion batteries with stable cycling performance. Considering its operational voltage range, it can also be used as a positive electrode in non-aqueous systems.[8] All of the characteristics illustrated above show promising potential for $Na_{0.44}MnO_2$ as a positive electrode material for sodium-ion batteries targeting grid-scale applications.

Generally, $Na_{0.44}MnO_2$ can be synthesized via a hydrothermal route or solid-state reaction. These processes require extensive heat treatment to obtain crystalline materials, and they face difficulties in obtaining homogeneous products due to the challenge of process control.[5–11] To reduce energy consumption during production, and improve homogeneity of the product, we use spray pyrolysis for synthesizing such multi-component metal oxides. Spray pyrolysis, a promising development for larger scale synthesis in industry, requires shorter residence times in the reactor, eliminates further washing and purification steps, and achieves excellent batch-to-batch reproducibility.[12–14] The literature shows that a variety of simple or complex metal/metal oxides can be synthesized via spray pyrolysis and related spray technologies, at multiple scales.[15–18] However, to the best of the authors' knowledge, spray pyrolysis have not been applied to the synthesis of tunnel structure sodium manganese oxide.

https://doi.org/10.1557/mrc.2017.4 Published online by Cambridge University Press

A single-step, facile spray pyrolysis process is used in this work for the synthesis of sodium-ion battery cathode materials. The composition and performance of tunnel structure sodium manganese oxide synthesized via spray pyrolysis are evaluated for the first time. The results indicate that $Na_{0.44}MnO_2$ can be successfully produced via a scalable and reproducible method without sacrificing electrochemical performances.

Experimental

The precursor solutions were prepared by dissolving $NaNO_3$ and $Mn(NO_3)_2{\cdot}4H_2O$ (Sigma Aldrich, MO, USA) in deionized water at the desired Na/Mn ratio. Samples A, B, and C represent materials synthesized from precursor with Na/Mn ratios equaling 0.44, 0.50, and 0.56, respectively. Total dissolved salt concentration was fixed at 2.5 mol/L (M). An aerosol flow reactor (AFR) was used for spray pyrolysis synthesis. Detailed information and the experimental scheme can be found in a previous publication from this group.[19] The preheater and furnace reactor temperatures were controlled at 200 and 575 °C, respectively. The as-synthesized samples after AFR were annealed for 2 h at 800 °C, which is commonly used in the literature.[5,7] The samples were also tested with annealing temperatures of 700 and 900 °C. The phase purity and the electrochemical performances were inferior to the ones shown by the samples annealed under 800 °C (results not shown here). The annealed powders were characterized by x-ray diffraction (XRD) using an x-ray diffractometer (Bruker D8 Advance, Bruker Corporation, Karlsruhe, Germany) at a scan rate of 0.04 °/s between 10° and 70° 2θ. Quantitative phase analysis (QPA) was performed with Bruker TOPAS 5 software. The traditional Rietveld method was used and $Na_4Mn_9O_{18}$ (space group: *Pbam*), Mn_2O_3 (space group: *Cmcm*), $Na_{0.67}MnO_2$ (space group: *Ia*-3) were used as identified phases. Particle morphology was examined with an FEI Nova 2300 field-emission scanning electron microscopy (SEM—FEI Company, OR, USA).

For cathode film fabrication, firstly, the cathode slurry was prepared by mixing 10 wt% polyvinylidene fluoride binder solution (Kureha Corp., Tokyo, Japan), 10 wt% C45 conductive carbon black (Imerys, Bodio, Switzerland), and 80 wt% active material in 1-methyl-2-pyrrolidinone (NMP—Sigma Aldrich). The active material loading density was between 2.5 and 4.0 mg/cm^2. The slurry was cast into a 15 µm film using a doctor blade. The film was dried at 40 °C for 1 h and at 130 °C for 2 h.

The 2032-type coin cells (Hohsen Corp., Osaka, Japan) were assembled in an argon-filled glove box (O_2 and H_2O level below 0.1 ppm) and were used for electrochemical performance tests. Half-cells were assembled using pure sodium anodes (Alfa Aesar, MA, USA) and 3501 Celgard membranes (Celgard LLC, NC, USA). The electrolyte solution was 1 M $NaClO_4$ in polypropylene carbonate (PC—Sigma Aldrich) with 2 vol% fluoroethylene carbonate (FEC—Alfa Aesar). Cycling and rate capability tests were performed using an MTI-BST8-WA battery tester at 22 °C. All cell tests were performed between 2.0 and 4.0 V (1C = 120 mAh/g).

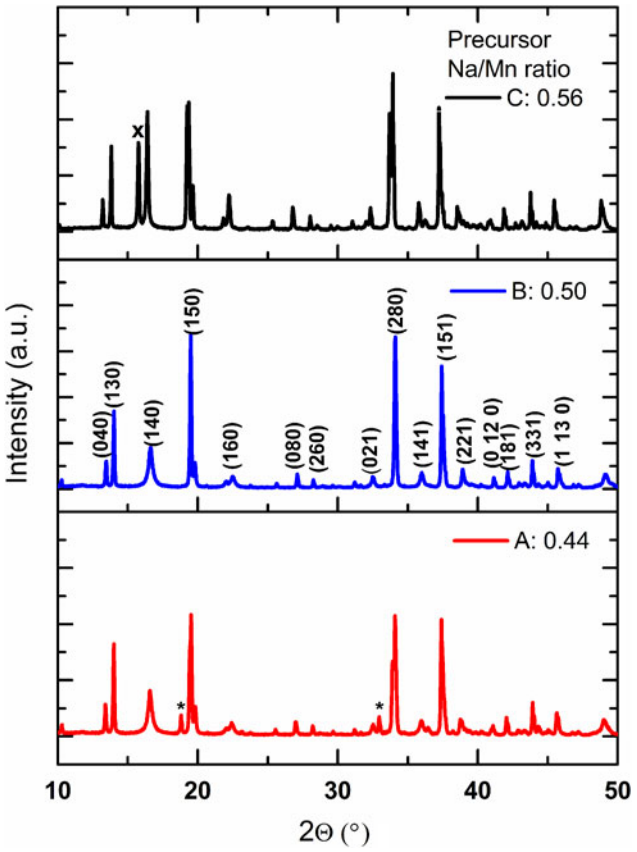


Figure 1. Comparison of the XRD patterns of tunnel structure sodium manganese oxides with different Na/Mn ratios in the precursor. (Samples A, B, and C represent precursor Na/Mn ratios equaling 0.44, 0.50, and 0.56, respectively.)

Results and discussion

The XRD patterns of materials with different precursor Na/Mn ratios are shown in Fig. 1. All samples crystallize mainly in an octahedral lattice cell (*Pbam* space group). However, well-crystallized, phase pure $Na_{0.44}MnO_2$ can only be seen in sample B, where the precursor Na/Mn ratio equals to 0.50. The Mn_2O_3 phase (marked as *) indicates sodium deficiency in sample A due to sodium loss under high temperature, while the excess sodium in sample C leads to a $Na_{0.67}MnO_2$ phase (marked as *x*).[8,20] The precursor Na/Mn ratio needs to be

Table I. Rietveld quantitative phase analysis of tunnel structure sodium manganese oxide.

Sample	$Na_4Mn_9O_{18}$ (wt%)	Mn_2O_3 (wt%)	$Na_{0.67}MnO_2$ (wt%)
A	93.62	6.38	0
B	99.58	0.37	0.04
C	88.24	1.71	10.06

https://doi.org/10.1557/mrc.2017.4 Published online by Cambridge University Press

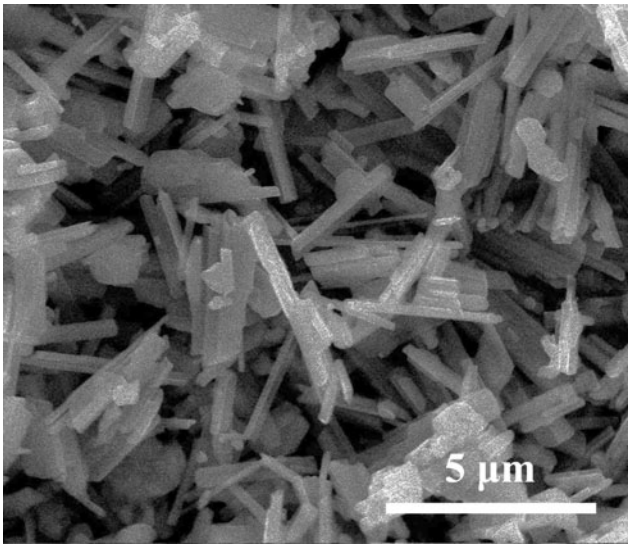


Figure 2. Morphology of tunnel structure sodium manganese oxide synthesized via spray pyrolysis, as observed by SEM at 20,000× magnification.

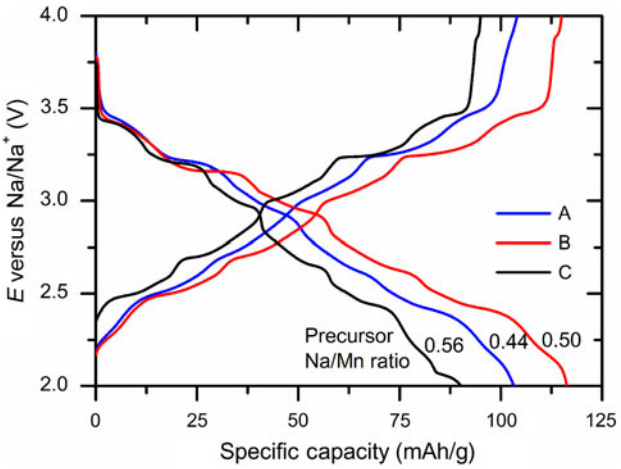


Figure 3. Second cycle voltage profiles of tunnel structure sodium manganese oxides with different Na/Mn ratios in the precursor. (Samples A, B, and C represent precursor Na/Mn ratios equaling 0.44, 0.50, and 0.56, respectively.)

well controlled to synthesize phase pure $Na_{0.44}MnO_2$. The ability to deliver uniform composition in both local and bulk scales in spray pyrolysis, shown in previous works,[12–14,21] demonstrates the advantage of this technique in synthesizing this material.

Rietveld quantitative phase analysis of the three samples is shown in Table I. Sample B demonstrates pure tunnel structure sodium manganese oxide. The results matched those indicated by the XRD patterns.

Figure 2 shows the morphology of tunnel structure sodium manganese oxide particles synthesized by spray pyrolysis (sample B). All three materials demonstrate similar morphology regardless of precursor Na/Mn ratios. After decomposition and annealing, the particles transformed to a rod-like morphology. The length of the particles is between 2 and 3 µm and the width ranges from 350 to 450 nm, as estimated from the SEM images. The morphology of the particles matches that described by other groups.[5,6]

The second cycle voltage profiles of sodium manganese oxides are demonstrated in Fig. 3. Voltage plateaus representing tunnel structure sodium manganese oxide material can be clearly observed at 2.5, 2.7, 3.0, 3.3, and 3.5 V for all three materials. Active Na^+ ions in the S-shaped tunnel are deserted/inserted reversibly between Na range of 0.22 (charged) and 0.66 (discharged), while the sodium ions located in the smaller tunnel remain inactive.[5] Sample B was able to

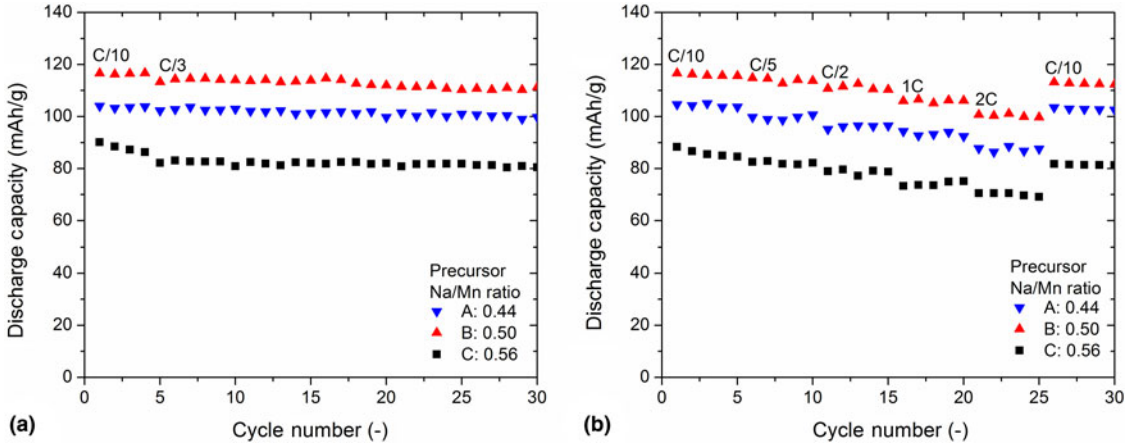


Figure 4. Comparison of (a) cycling and (b) rate capability of tunnel structure sodium manganese oxides with different Na/Mn ratios in the precursor. (Samples A, B, and C represent precursor Na/Mn ratios equaling 0.44, 0.50, and 0.56, respectively.)

https://doi.org/10.1557/mrc.2017.4 Published online by Cambridge University Press

deliver a discharge capacity of 115 mAh/g, which is 95% of the theoretical capacity of $Na_{0.44}MnO_2$.

Figure 4(a) compares cycle performances of the three sodium manganese oxides. The cells are cycled under C/10 for the first four cycles and C/3 for the remainder of the test. Sample B maintains the highest capacity of 110 mAh/g after 30 cycles due to its superior phase purity, while samples A and C deliver 100 and 81 mAh/g, respectively. The rate capabilities of different samples are also compared in Fig. 4(b). Cycling rates are increased every five cycles from C/10 up to 2C and then returned to C/10. $Na_{0.44}MnO_2$ synthesized via spray pyrolysis demonstrates good rate performance, as sample B shows 105 and 100 mAh/g under 1C and 2C, respectively. All testing cycles in Fig. 4 demonstrate coulombic efficiencies above 99%. The electrochemical performance of $Na_{0.44}MnO_2$ synthesized via spray pyrolysis is as good as that obtained by other traditional methods, such as solid-state synthesis and hydrothermal synthesis,[6,7] but the process is scalable and maintains product uniformity as it is scaled up. Both the XRD and cycling and rate comparison point out the importance of an optimal Na/Mn ratio. A few percentage points difference leads to significant changes in phase purity and electrochemical performance. For spray pyrolysis, 13.6% excess sodium is needed to achieve optimal $Na_{0.44}MnO_2$.

Summary

Tunnel structure sodium manganese oxides were synthesized via spray pyrolysis. The Na/Mn ratio in the precursor was altered between 0.44, 0.50, and 0.56. Among the materials, the sample that was produced with a Na/Mn precursor ratio of 0.50 shows phase pure $Na_4Mn_9O_{18}$ structure and delivers optimal electrochemical performance. A discharge capacity of 115 mAh/g is reached in the first cycle and the material also demonstrates good cycleability and rate performance.

This work points out the importance of optimizing composition of materials with complex stoichiometry in order to reach maximum performance. The capability of spray pyrolysis to deliver uniform composition throughout the material allows us to examine the effect of different stoichiometry within only a few percentage points accurately. As previous works have noted, this advantage of product uniformity is true even for large-scale spray pyrolysis, which would be critical for tunnel structure sodium manganese oxide when implemented for large-scale energy storage systems.

Acknowledgments

The authors would like to thank Dr. Pratim Biswas for the use of his glovebox. The authors are grateful to Dr. Naoaki Yabuuchi from Tokyo Denki University for his helpful discussions on sodium-ion cell fabricating. The electron microscopy facility used in this work was supported by the Nano Research Facility (NRF) at Washington University in St. Louis.

References

1. B.L. Ellis and L.F. Nazar: Sodium and sodium-ion energy storage batteries. *Curr. Opin. Solid State Mater. Sci.* **16**, 168 (2012).
2. V. Palomares, P. Serras, I. Villaluenga, K.B. Hueso, J. Carretero-Gonzalez, and T. Rojo: Na-ion batteries, recent advances and present challenges to become low cost energy storage systems. *Energy Environ. Sci.* **5**, 5884 (2012).
3. K. Kubota, N. Yabuuchi, H. Yoshida, M. Dahbi, and S. Komaba: Layered oxides as positive electrode materials for Na-ion batteries. *MRS Bull.* **39**, 416 (2014).
4. M.D. Slater, D. Kim, E. Lee, and C.S. Johnson: Sodium-ion batteries. *Adv. Funct. Mater.* **23**, 947 (2013).
5. F. Sauvage, L. Laffont, J.M. Tarascon, and E. Baudrin: Study of the insertion/deinsertion mechanism of sodium into $Na_{0.44}MnO_2$. *Inorg. Chem.* **46**, 3289 (2007).
6. E. Hosono, T. Saito, J. Hoshino, M. Okubo, Y. Saito, D. Nishio-Hamane, T. Kudo, and H. Zhou: High power Na-ion rechargeable battery with single-crystalline $Na_{0.44}MnO_2$ nanowire electrode. *J. Power Sources* **217**, 43 (2012).
7. L.W. Zhao, J.F. Ni, H.B. Wang and L.J. Gao: $Na_{0.44}MnO_2$-CNT electrodes for non-aqueous sodium batteries. *RSC Adv.* **3**, 6650 (2013).
8. Y. Wang, J. Liu, B. Lee, R. Qiao, Z. Yang, S. Xu, X. Yu, L. Gu, Y.-S. Hu, W. Yang, K. Kang, H. Li, X.-Q. Yang, L. Chen, and X. Huang: Ti-substituted tunnel-type $Na_{0.44}MnO_2$ oxide as a negative electrode for aqueous sodium-ion batteries. *Nat. Commun.* **6**, 6401 (2015).
9. F. Bi, Z. Xuan, and W. Yaping: High-rate performance electrospun $Na_{0.44}MnO_2$ nanofibers as cathode material for sodium-ion batteries. *J. Power Sources* **310**, 102 (2016).
10. S.L. Bai, J.L. Song, Y.H. Wen, J. Cheng, G.P. Cao, Y.S. Yang, and D.Q. Li: Effects of zinc and manganese ions in aqueous electrolytes on structure and electrochemical performance of $Na_{0.44}MnO_2$ cathode material. *RSC Adv.* **6**, 40793 (2016).
11. M.W. Xu, Y.B. Niu, C.J. Chen, J. Song, S.J. Bao, and C.M. Li: Synthesis and application of ultra-long $Na_{0.44}MnO_2$ submicron slabs as a cathode material for Na-ion batteries. *RSC Adv.* **4**, 38140 (2014).
12. M. Lengyel, D. Elhassid, G. Atlas, W.T. Moller, and R.L. Axelbaum: Development of a scalable spray pyrolysis process for the production of non-hollow battery materials. *J. Power Sources* **266**, 175 (2014).
13. T. Ogihara, T. Kodera, K. Myoujin, and S. Motohira: Preparation and electrochemical properties of cathode materials for lithium ion battery by aerosol process. *Mater. Sci. Eng. B* **161**, 109 (2009).
14. Y.J. Hong, J.H. Kim, M.H. Kim, and Y.C. Kang: Electrochemical properties of $0.3Li_2MnO_3{\cdot}0.7LiNi_{0.5}Mn_{0.5}O_2$ composite cathode powders prepared by large-scale spray pyrolysis. *Mater. Res. Bull.* **47**, 2022 (2012).
15. D.S. Jung, T.H. Hwang, S.B. Park, and J.W. Choi: Spray drying method for large-scale and high-performance silicon negative electrodes in Li-ion batteries. *Nano Lett.* **13**, 2092 (2013).
16. Z. Sadeghian: Large-scale production of multi-walled carbon nanotubes by low-cost spray pyrolysis of hexane. *New Carbon Mater.* **24**, 33 (2009).
17. K.Y. Jung, J.H. Lee, H.Y. Koo, Y.C. Kang, and S. Bin Park: Preparation of solid nickel nanoparticles by large-scale spray pyrolysis of $Ni(NO3)_2{\cdot}6H_2O$ precursor: effect of temperature and nickel acetate on the particle morphology. *Mater. Sci. Eng. B* **137**, 10 (2007).
18. K. Okuyama, M. Abdullah, I.W. Lenggoro, and F. Iskandar: Preparation of functional nanostructured particles by spray drying. *Adv. Powder Technol.* **17**, 587 (2006).
19. M. Lengyel, G. Atlas, D. Elhassid, P.Y. Luo, X. Zhang, I. Belharouak, and R.L. Axelbaum: Effects of synthesis conditions on the physical and electrochemical properties of $Li_{1.2}Mn_{0.54}Ni_{0.13}Co_{0.13}O_2$ prepared by spray pyrolysis. *J. Power Sources* **262**, 286 (2014).
20. Y.U. Jeong and A. Manthiram: Synthesis of $Na_xMnO_{2+\delta}$ by a reduction of aqueous sodium permanganate with sodium iodide. *J. Solid State Chem.* **156**, 331 (2001).
21. M. Lengyel, K-Y. Shen, D.M. Lanigan, J.M. Martin, X. Zhang, and R.L. Axelbaum: Trace level doping of lithium-rich cathode materials. *J. Mater. Chem. A* **4**, 3538 (2016).

https://doi.org/10.1557/mrc.2017.4 Published online by Cambridge University Press